2008 International Symposium on Nonlinear Theory and its Applications
NOLTA'08, Budapest, Hungary, September 7-10, 2008

Assessing the local stability of action potential propagation in cardiac tissue

Enno de Lange† and Jan P. Kucera

Department of Physiology, University of Bern
Bühlplatz 5, 3012 Bern, Switzerland
†Email: delange@physio.unibe.ch

Abstract—We devised a method to assess the local stability of action potential propagation in cardiac tissue using coupled iterated maps of propagation velocity and action potential duration. The method is illustrated using simulations of propagation in chains of Luo-Rudy cell models and electrophysiological recordings from patterned strands of cultured neonatal rat ventricular myocytes. We de-stabilize conduction by decreasing extracellular potassium concentration. A first-order linear model gives a good description of the observed dynamics for both the control and the low extracellular potassium situation.

1. Introduction

In cardiac electrophysiology the term "restitution" designates the rate-dependent behavior of the action potential (AP). Restitution models describe cardiac dynamics using iterated maps. Since the pioneering work of Nolasco and Dahlen [8], who first described the relation between AP duration (APD) and diastolic interval (DI) in cardiac tissue as a first-order iterated map, several additional restitution models have been proposed. The logical extension was to model propagation by restitution of conduction velocity (CV) [2]. Later, observations that the stability of AP generation in single cells does not always depend on the slope of the APD restitution model of Nolasco and Dahlen have led to the introduction of higher-order APD restitution maps [1]. Most recently, models have been proposed that incorporate intracellular calcium dynamics in the mechanisms of APD restitution [9].

In this paper we present a method to assess restitution characteristics by measuring transfer functions of the intervals between successive AP wavefronts (interbeat intervals; IBIs). We first give a closed form expression of the transfer function of IBIs between two sites in cardiac tissue (Sec. 2), based on first-order APD and CV restitution. From a systems identification point of view, an input signal incorporating random variations with a broad spectrum is an efficient signal to identify the underlying dynamics of the system. This then makes a signal with a Gaussian variation around some mean basic cycle length (BCL) an obvious choice as an input signal to measure the transfer functions in simulations and in vitro (Sec. 3). We illustrate the method by determining the transfer functions of IBI in simulations of a strand of Luo-Rudy model cells (Sec. 4.1) and in cultured strands of rat ventricular myocytes (Sec. 4.2). Finally we show that our method allows estimation of APD restitution properties without measuring APD (Sec. 4.3).

2. Theory: Cardiac restitution as a transfer function

We hypothesized that for our cultures of rat ventricular myocytes, linear first-order APD and CV restitution is an appropriate model to predict the observed dynamics. We consider regularly paced cardiac tissue with a series of pulses with certain IBIs (see Fig. 1).

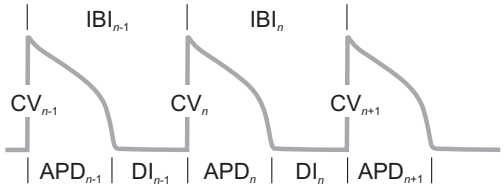

Figure 1: Relation between the different variables describing the AP.

Calling the time series of subsequent APDs a, the time series of DIs d and the time series of IBIs t, the first order restitution relation of APD is

$$a_{n+1} = f(d_n). \tag{1}$$

Under periodic stimulation with IBI=BCL, this relation can be linearized around its working point. We call the derivative of (1) in the working point α.

Using the fact that, by definition, $t_n = d_n + a_n$, and writing δd and δa for small variations of DI and APD around the working point, we obtain the linearized APD restitution relation from (1) as $\delta t_{n+1} - \delta d_{n+1} = \alpha\, \delta d_n$. Applying the Z-transform to this relation, with T the Z-transform of t and D the Z-transform of d, and solving for D/T, gives the transfer function for the evolution of the variations of the DI as a function of variations δt of the IBI around its working point:

$$H_{t\to d}(z) = \frac{D(z)}{T(z)} = \frac{z}{z+\alpha}. \tag{2}$$

The first-order system relating DI to IBI has a pole at $-\alpha$ and a zero at the origin.

Now suppose that AP wavefronts are passing through cardiac tissue and we measure the IBIs at two sites sufficiently far away from the boundaries such that we can ignore boundary effects. We assume a first-order difference

relation between CV—denoted by the variable c—and the previous DI:

$$c_{n+1} = g(d_n). \tag{3}$$

This relation can again be linearized for a specific working point with IBI=BCL. We call the derivative of (3) in the working point γ.

Now consider the elements of the time series c, d and t to be functions of the distance x along the path between the two measurement sites, with $x = 0$ at the first measurement site and $x = L$ at the second measurement site. We suppose that the tissue is homogeneous, i.e., that APD and CV restitution do not depend on x. The conduction time to cover an infinitesimal segment of length $\mathrm{d}x$ is $\mathrm{d}x/c_n(x)$ for the n^{th} AP and $\mathrm{d}x/c_{n+1}(x)$ for the $n+1^{\mathrm{st}}$ AP, and the IBI between those APs changes by

$$\frac{\mathrm{d}t_n(x)}{\mathrm{d}x} = \frac{1}{c_{n+1}(x)} - \frac{1}{c_n(x)}. \tag{4}$$

Using the chain rule and (3), we see that the derivative of $1/c_{n+1}(x) = 1/g(\delta d_n)$ in the working point is $-\gamma/c_{ss}^2$, with c_{ss} the steady state CV. Therefore the linearization of (4) around the working point is:

$$\frac{\mathrm{d}t_n(x)}{\mathrm{d}x} = -\frac{\gamma}{c_{ss}^2}\left(\delta d_n - \delta d_{n-1}\right) \tag{5}$$

The formulation of (5) is a distributed parameter model [5]. By applying the appropriate transform, a transfer function between different points x can be obtained, which is an analytic function of z, though not rational as the traditional transfer function. Applying the Z-transform to (5) and using (2), we obtain the ordinary differential equation

$$\begin{aligned} \frac{\mathrm{d}T(z,x)}{\mathrm{d}x} &= \frac{\gamma}{c_{ss}^2}\left(z^{-1}-1\right)D(z,x) \\ &= \frac{\gamma}{c_{ss}^2}\frac{1-z}{z}H_{t\to d}(z)T(z,x). \end{aligned} \tag{6}$$

In this equation we used the APD restitution transfer function $H_{t\to d}$, which, as mentioned before, we suppose to be independent of x. By integrating (6) we obtain the transfer function of interbeat intervals for propagation between the site $x = 0$ and the site $x = L$ as:

$$H_t(z) = \exp\left(\frac{\gamma L}{c_{ss}^2}\frac{1-z}{\alpha+z}\right). \tag{7}$$

Note that this relation gives an estimation of both γ and α. Since H_t can be obtained from extracellular measurements of activation times, this gives a way of estimating APD restitution without actually measuring APD.

3. Methods

3.1. Numeric simulations using the Luo-Rudy ionic model

Conduction was simulated in a 1 cm long fiber of 100 Luo-Rudy model cells [6]. To obtain CVs and APDs in the range of those observed in cultures of neonatal rat ventricular myocytes, the maximal sodium current conductance (g_{Na}) and the slow inward current conductance (g_{si}) were reduced to 8 and 0.04 mS/cm^2, respectively [10, 7]. Further details about the model and the numerics are provided in a previous publication [7].

The fiber was paced at one extremity (see Sec.3.3). Activation times were defined by depolarization to -35 mV during the AP upstroke and APD was measured at repolarization to -80 mV. IBIs were established at $x = 0.25\,\mathrm{cm}$ (input) and $x = 0.75\,\mathrm{cm}$ (output).

3.2. In vitro preparations

Patterned strands of ventricular myocytes (width: 150 μm) from 1-2 days old Wistar rats were prepared and grown on microelectrode arrays as described previously [4]. The strands were grown on rows of 6 or 12 electrodes (spacing: 1.2 or 0.5 mm, respectively) or on meandering paths of 60 electrodes (spacing 1.2 mm), with one stimulation dipole at the beginning. Experiments were performed on 3-5 days old cultures in Hanks' balanced salts solution (HBSS) and at 36 °C. In certain experiments, the extracellular potassium concentration ($[K^+]_o$) of the HBSS was reduced to 1.5 mmol/L. Signals were sampled at 10 kHz and activation times were defined at the occurrence of the minimum of their first derivative [4].

3.3. Pacing protocol

The stimulation protocol used in this work is shown in Fig. 2. To establish steady state conditions in the model

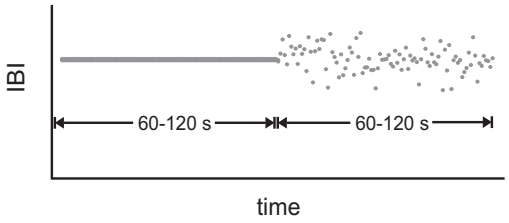

Figure 2: Stochastic stimulation protocol.

as well as in the experiments, the cell strands were initially paced at a given BCL until all transients had stabilized. Subsequently stochastic pacing was applied: IBI was varied randomly around BCL with a Gaussian distribution characterized by a predefined standard deviation σ. The stochastic protocol was applied for 256 cycles in the simulations or during 1-2 min in vitro.

3.4. Automatic fitting of the transfer functions

There exists systematic methods to fit distributed parameter models like (5) to data [5], but they are usually quite elaborate. Since (5) is relatively simple, with only two parameters, we used the ready-implemented brute-force optimization algorithms from the MATLAB Optimization

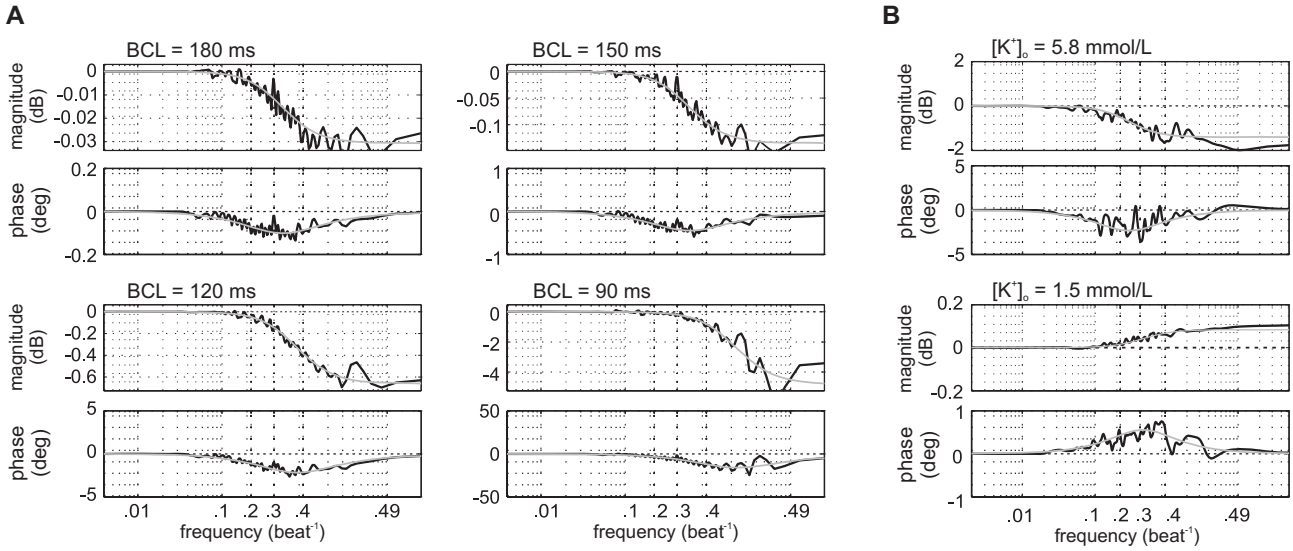

Figure 3: *(A)* Transfer functions of Luo-Rudy model strands at different BCLs. *(B)* Transfer functions of cultured strands under control conditions (*top*) and in low $[K^+]_o$ (*bottom*), at BCL=150 ms, $L = 0.96\,\mathrm{cm}$.

Toolbox. We used the line-search algorithm, with initial parameter values randomly distributed in the interval of plausible values. The validity of the approach was verified by performing multiple repetitions of the optimization, with different initial parameter values, which did not lead to a significant change in the outcome.

4. Results

We estimated transfer functions of IBIs in simulations of a strand of Luo-Rudy model cells as well as in extracellular measurements of cultured strands by computing the ratio of the Welch cross power spectral density of the output and input to the power spectral density of the input. We then fit the transfer functions with (5). The transfer functions are shown in Fig. 3 in the form of Bode plots.

The scale of the frequency-axes of the Bode plots is skewed by considering the transfer function $H(z)$ along the contour $z = e^{j2\pi f}$ in the z plane. The contour is then mapped to the (positive) imaginary axis. This transformation allows Bode plots of discrete-time systems to be constructed and interpreted in the same way as those of continuous-time system, e.g., poles cause a 20 dB/decade decrease of the slope of the transfer function and zeros inside the unit circle a 20 dB/decade increase [3].

4.1. Transfer functions of Luo-Rudy model strands

The black lines in panel *A* of Fig. 3 show the computed transfer functions for the simulations of the Luo-Rudy model strand. The stochastic protocol was applied for four different BCLs. The gray lines are the fits of (5) to the black curves.

For decreasing BCL the pole in the transfer functions shifts to higher frequencies, as is evident from the rightward shift of the dropoff of the transfer function. This corresponds to α approaching unity for decreasing BCL, as is usual.

On the other hand, the attenuation at higher frequencies increases for lower BCLs. This corresponds to increasing γ. The physiological interpretation is that at pacing rates closer to the maximal possible rate, CV restitution attenuates higher frequencies and therefore any deviation from BCL. This stabilizes conduction at higher beat rates, counteracting the destabilizing effect of APD restitution at low BCL.

4.2. Transfer functions of cultured cell strands

It is clear that a possibly dangerous situation can emerge when γ becomes negative. In this case the higher frequencies are amplified, instead of attenuated. This situation can occur when extracellular potassium concentration is decreased. Figure 3, *B* shows the transfer functions of IBI in strands of rat ventricular myocytes as measured under normal conditions ($[K^+]_o$=5.8 mmol/L) and in low extracellular potassium ($[K^+]_o$=1.5 mmol/L).

It can be seen that the fits of (5) (gray lines) also form a good approximation of the measured transfer functions (black traces) for the experimental results. For low extracellular potassium, higher frequencies are amplified and the phase is non-minimal. The amplification is maximal at half of the BCL, which is the frequency of alternans, a phenomenon which is considered a risk factor for sudden cardiac death.

4.3. Using the transfer functions to predict the slope of APD restitution

The slope of the first-order APD restitution is considered an important indicator for alternans. In vivo as well as in our preparations it is difficult to measure APD directly, but the transfer functions presented in this work can be deduced from two-site measurements of activation times along the axis of propagation. The transfer functions can in principle give information about both APD and CV restitution (both α and γ appear in (5)). To evaluate the precision of the assessment of APD restitution by extraction of α from the transfer function, we used our simulations, in which we do have access to APD.

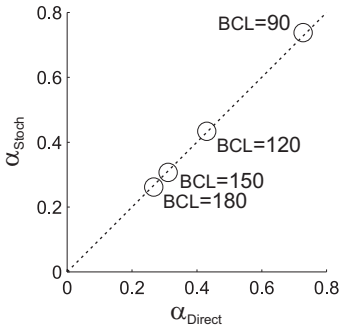

Figure 4: Comparison between APD restitution slopes in Luo-Rudy model strands as measured directly and as derived from the fitted transfer functions.

Figure 4 shows a comparison between the APD restitution slopes α as extracted from the transfer functions by fitting (5) as shown in Fig. 3, A (α_{Stoch}) and as measured directly (α_{Direct}). All four points lie almost perfectly on the line $\alpha_{\text{Stoch}} = \alpha_{\text{Direct}}$ (linear regression: $\alpha_{\text{Stoch}} = 1.0335\alpha_{\text{Direct}} + 0.0137$ with $r > 0.9999$). This shows that in simulations of Luo-Rudy model strands the APD restitution slope can be accurately determined from the transfer function.

5. Conclusions

The propagation of action potentials through cardiac tissue can be represented by a transfer function of a linear distributed parameter system. This transfer function can be conveniently obtained from measurements of activation times at two different sites in the tissue. The transfer function then gives information about the restitution properties of cardiac tissue, which are important for the stability of conduction and therefore for the risk assessment of arrhythmias and sudden cardiac death.

We propose a stochastic pacing protocol to measure transfer functions. The advantage of such a stimulation protocol as compared to more traditional protocols (which typically focus on directly measuring dynamical aspects like the slope of restitution functions) is that it gives more information about the dynamics, it can be shorter in duration, and it is power-efficient.

We showed that a transfer function including only first-order restitution characteristics fits the measured transfer functions reasonably well, in both our simulations and experiments. Using the simulations we show that the first-order transfer function, which can be obtained without explicitly measuring APD, can give a good estimation of APD restitution slopes.

Acknowledgments

This work was supported by the Swiss National Science Foundation (grants 3100A0-100285 and 310000-120514).

References

[1] J. W. Cain, E. G. Tolkacheva, D. G. Schaeffer, and D. J. Gauthier. Rate-dependent propagation of cardiac action potentials in a one-dimensional fiber. *Phys Rev E*, 70(6 Pt 1):061906, 2004.

[2] M. Courtemanche, L. Glass, and J.P. Keener. Instabilities of a propagating pulse in a ring of excitable media. *Phys Rev Lett*, 70(14):2182–2185, 1993.

[3] R.A. Gabel and B.J. Smith. Bode plot analysis of linear discrete-time systems. *IEEE Trans. on Acoustics, Speech and Signal Processing*, 23:525–529, 1975.

[4] A. A. Kondratyev, J. G. Ponard, A. Munteanu, S. Rohr, and J. P. Kucera. Dynamic changes of cardiac conduction during rapid pacing. *Am J Physiol Heart Circ Physiol*, 292(4):H1796–H1811, 2007.

[5] C.S. Kubrusly. Distributed parameter system identification – a survey. *Int. J. Control*, 26:595–605, 1977.

[6] C. H. Luo and Y. Rudy. A model of the ventricular cardiac action potential. depolarization, repolarization, and their interaction. *Circ Res*, 68(6):1501–1526, 1991.

[7] A. Munteanu, A.A. Kondratyev, and J.P. Kucera. Analysis of damped oscillations during reentry: a new approach to evaluate cardiac restitution. *Biophys J*, 94(3):1094–1109, Feb 2008.

[8] J. B. Nolasco and R. W. Dahlen. A graphic method for the study of alternation in cardiac action potentials. *J Appl Physiol*, 25(2):191–196, 1968.

[9] Z. Qu, Y. Shiferaw, and J. N. Weiss. Nonlinear dynamics of cardiac excitation-contraction coupling: an iterated map study. *Phys Rev E*, 75:011927, 2007.

[10] Z. Qu, J. N. Weiss, and A. Garfinkel. Cardiac electrical restitution properties and stability of reentrant spiral waves: a simulation study. *Am J Physiol Heart Circ Physiol*, 276:H269–H283, 1999.